International Journal of Recent Trends in Engineering & Research (IJRTER)
Conference on Recent Trends in Electrical and Electronics Engineering (RTEEE '19)
Special Issue; March- 2019 [ISSN: 2455-1457]
DOI: 10.23883/IJRTER.CONF.20190304.005.RCLXE

SPECTRAL UNMIXING BASED ON JOINT SPARSITY AND TOTAL VARIATION USING REMOTE SENSING DATA

[1]J.M. Andiria Joslin,[2] R. Ablin

[1]UG Student, [2] Assistant Professor, Dept. of ECE,
Arunachala College of Engineering for Women

Abstract—Hyperspectral imaging belongs to a class of technique called spectral imaging or spectral analysis. The objective of hyperspectral imaging is to find the spectrum for each pixel Present in the image of a scene. Hyperspectral unmixing is an emerging topic in hyperspectral image analysis to distinguish the materials present in an image and thereby finding the proportion of each material in an image. The distinct materials are called as end members and proportion values are called as abundance maps. Hyperspectral unmixing is an important technique for estimating fraction of different land cover types from remote sensing imagery. It is the process of estimating constituent endmembers and their fractional abundances present at each pixel in a hyperspectral image. A hyperspectral image is often corrupted by several kinds of noise. Joint Sparsity and Total variation (JSTV) addresses the hyperspectral unmixing problem in a general scenario that considers the presence of mixed noise. The Joint sparsity has been formulated to exploit the abundance maps. A total-variation based regularization has also been utilized for modeling smoothness of abundance maps. The split-Bregman technique has been utilized to derive an algorithm for solving resulting optimization problem. Results indicate that the proposed joint sparsity and total variation methods are able to successfully perform unmixing on synthetic data and real hyperspectral imagery while preserving endmember spatial information with smooth abundance maps.

***Index Terms*-Hyperspectral Unmixing, Joint-Sparsity, Split-Bregman ,Total Variation, Mixed-Noise**

I.INTRODUCTION

Hyperspectral imaging provides enhanced classification, detection, and identification performance with respect to standard imaging systems, by utilizing the high amount of spectral information for each pixel. It is a problem of identifying endmembers and their fractional abundances present at every pixel in a hyperspectral image.The term endmember refers to various materials that may be directly or indirectly present in a hyperspectral image. The term direct presence refers to the existence of pure pixels and indirect presence refers to mixed pixels.

A pixel in a satellite image corresponds to an extensive spatial area on earth. This spatial region constituting that pixel may be covered by a single object or multiple objects. If the area covered by a pixel constitutes a single object then such a pixel is called pure pixel otherwise it is called mixed pixel. The term fractional abundance indicates the percentage of a particular endmember present at a pixel. Thus, abundance map shows the distribution of a particular endmember over a region. The pure pixels have the fractional abundance of one whereas mixed pixels have fractional abundance between zero and one.

Hyperspectral unmixing has applications in various domains such as geology, agriculture [1], environmental studies, biology [2], etc. The abundance maps are often used as feature vectors [3] in several image processing and pattern recognition related applications of hyperspectral images. Hyperspectral unmixing is also used in denoising [4], data fusion [5], and super-resolution [6] related applications.

Often hyperspectral images are corrupted by some kinds of noise such as Gaussian noise, impulse noise, shot noise, horizontal or vertical line strips, etc. Gaussian noise mostly occurs during image acquisition process due to poor lighting, dark current or sensor noise. Horizontal line strips often occur in images captured by whisk-broom kind of sensors that have rotating mirrors perpendicular to the flight direction. Vertical line strips mostly occur in images captured by push-broom kind of sensors which capture scene along the flight direction. Shot noise occurs due to some defective pixels. It is desirable to do unmixing of hyperspectral images even when they are corrupted by one or several of these kinds of noise. This problem of unmixing in the presence of mixed noise can be approached by firstly applying a denoising algorithm followed by the unmixing algorithm.This work directly recovers the abundance map in the presence of mixed noise. There are studies such as [4], [12] that also perform unmixing in the presence of noise. This work is different from these existing methods in terms of both the noise model and the solution approach

This model allows us to formulate the linear hyperspectral unmixing problem that explicitly account for both Gaussian and sparse noise. The term sparse noise corresponds to the noise that affects few pixels in the image. It includes line strips, shot noise as well as impulse noise. The total number of endmembers available from different spectral libraries (e.g. the USGS library) are huge, but only a few of these endmembers are present in a given hyperspectral image.

This observation can be modeled as joint-sparse[15] regularization on abundance maps. Natural images often exhibit high spatial correlation implying that pixels having the same spectral signature may be present in the neighborhood. This observation can be modeled as total-variation [16] regularization on abundance maps. Thus, this work proposes a hyperspectral unmixing algorithm that

DOI: 10.23883/IJRTER.CONF.20190304.005.RCLXE

utilize generic noise model and explores both joint sparsity and spatial smoothness of abundance maps. The resulting optimization problem is solved using the split-Bregman based [17] technique.

Section II describes detailed problem formulation followed by section III describes the technique to solve proposed formulation. Section IV describes experimental results and section V concludes the paper with some future directions

II.PROBLEM DEESCRIPTION AND FORMULATION

This section describes how linear unmixing problem can be mathematically formulated as sparse recovery problem followed by proposed problem formulation.

A.*Notations*

Let I_n represents identity matrix of size n×n.The operation x = vec(X) represents vectorization operation on matrix X with columns appended whereas X = mat(x) represents its inverse operation. A hyperspectral data cube of size $m \times n \times b$ can be represented as a matrix of size $b \times p$ where b is the total number of bands and $p = m \times n$ is the total number of pixels in the image. $M \in R^{bxc}$ represents mixing matrix also called endmember matrix in which each column represents spectral signature of an endmember.

Let $\nabla = \begin{pmatrix} \nabla h \\ \nabla v \end{pmatrix}$ be total variation operator with ∇_h and ∇_v representing horizontal and vertical total vatiation operators respectively with $(\nabla_h X)_{i,j} = X_{i,j} - X_{i,j}$ and $(\nabla_v X)_{i,j} = X_{i,j} - X_{i,j}$ .The $\ell_{2,1}$ norm of a matrix $A \in R^{M \times N}$ is defined as

$$\|A\|_{2,1} = \sum_{i=1}^{M} |a| = \sum_{i=1}^{M} \sqrt{\sum_{j=1}^{N} |a|_{i,j}}$$

B. Problem Description

The linear unmixing problem for a pixel in the presence of Gaussian noise is represented as

$$Y = Ma + n, \quad \|a\|_1 = 1, \quad a_I \geq 0 \forall_i$$

where $y \in R^{bx1}$ is a pixel vector in b spectral bands, M is a mixing matrix with e number of endmembers as column vectors, $a \in R^{ex1}$ is called abundance vector that represents the fraction of each endmember used in the formation of that pixel, and n represents Gaussian noise which accounts for various external environmental factors. The constraint ||a|| = 1 represents abundance sum-to-one constraint to ensures that total contribution of each endmember in formation of a pixel is one. As it has been noticed in [7], [21], [22], all the endmembers present in a real hyperspectral image may not be available in the spectral library.

The observation that a pixel is mixture of very few endmembers as opposed to hundreds of available endmembers allow us to treat abundance vector a as sparse vector thus unmixing can be recast as compressed sensing [23], [24] problem :

$$\min \alpha \ \|y - Ma\|_2^2 \text{ subject to } \|a\|_0 \leq k$$

where k is the sparsity of a i.e.maximum number of nonzero elements of a.

It has been shown that under certain conditions solution of the NPhard problem (2) can be approximated by solving its convex surrogate ℓ_1-norm minimization problem

$$\min \alpha \ \|y - Ma\|_2^2 + \lambda \|a\|_1$$

The unmixing model in (1) can be extended for all the pixels as

$$Y = MA + N, \quad A \geq 0$$

where $Y \in R^{bxp}$ is a matrix with p pixels as column vectors, $A \in R^{exp}$ is sparse abundance matrix, N is Gaussian noise. This unmixing model can be though of as specialization of image denoising model :

$$Y = X + N$$

where $X \in R^{bxp}$ and X = MA is clean hyperspectral image which imply that unmixing can lead to denoising provided that mixing matrix is known.

C.Proposed Formulation

A real hyperspectral image may contain a mixture of Gaussian and sparse noise therefore, the mixed noise model for unmixing is considered for both types of noise. The usual unmixing model can be extended as

$$Y = MA + S + G, \ A \geq 0$$

here S and G represents sparse and Gaussian noise respectively.

The noise model assumes both Gaussian and sparse noise to be additive noise. Sparse noise accounts for horizontal or vertical line strips, shot noise and any impulse noise present in a hyperspectral image. All these kinds of noise are termed as sparse noise since they corrupt few pixels in a hyperspectral image.

$$\min_{A,S} \|Y - MA - S\|_F^2 + \lambda_1 \|A\|_{2,1} + \lambda_2 \|S\|_1$$

The first term is data fidelity term that is equivalent to minimizing the variance of Gaussian noise G = Y – MA – S. First regularization term is an $\ell_{2,1}$-norm minimization term on abundance matrix A which is also called joint-sparse regularization term. This term is based on the observation that in most hyperspectral images, a fewer endmembers are present compared to the available endmembers. The observation is mathematically modelled as joint-sparse regularization on matrix A with few non-zero rows, but each non-zero row is allowed to be dense.

DOI: 10.23883/IJRTER.CONF.20190304.005.RCLXE

The second regularization term corresponds to minimizing ℓ_1-norm of sparse noise matrix S.Here ℓ_1-norm is minimized due to modelling assumption that sparse noise affects few pixels in the image. As an alternative unmixing model the abundance maps can be considered as piece-wise smooth. The piece-wise smoothness can be modelled as total variation regularization.

$$\min_{A,S} \|Y - MA - S\|^2_F + \lambda_1 \|\nabla A^T\|_1 + \lambda_2 \|S\|_1$$

Here ∇ is two-dimensional total variation operator that applies total variation along both horizontal and vertical direction on a 2D image. The operator ∇ is applied on A^T because each abundance map is along rows of A.

$$\min_{A,S} \|Y - MA - S\|^2_F + \lambda_1 \|\nabla A^T\|_1 + \lambda_2 \|A\|_{2,1} + \lambda_3 \|S\|_1$$

Here λ_1, λ_2 and λ_3 are regularization parameters corresponding to total-variation term, joint-sparsity term, and sparse noise term respectively. These three models estimates sparse noise S as a byproduct of the proposed formulations.

Let X = MA be the clean image then we can get denoised image X = MA where A is the estimated abundance maps by solving. Along with generic noise model, both joint-sparsity as well as piecewise-smoothness of abundance maps were exploited. In the next section this problem was solved using the split-bregman technique.

III.PROPOSED METHOD

The proposed algorithm is split bregmen approach which utilizes both joint sparsity and total variation methods. The variable A is not separable in (8) therefore we utilize auxiliary variables P and Q to make the problem separable. Set $P = \nabla A^T$ and $Q = A$, then we get following constrained problem:

$$\text{Minimize}_{A,S,P,Q} \|Y - MA - S\|^2_F + \lambda_1 \|P\|_1 + \lambda_2 \|Q\|_{2,1} + \lambda_3 \|S\|_1$$

Subject to $P = \nabla A^T$
$Q = A,$

This problem can be re-written into unconstrained form by using two Bregman variables B1 and B2 to get

$$\text{Minimize}_{A,S,P,Q} \|Y - MA - S\|^2_F + \lambda_1 \|P\|_1 + \lambda_2 \|Q\|_{2,1} + \lambda_3 \|S\|_1$$
$$+\mu_1 \|P - \nabla A^T - B_1\|^2_F + \mu_2 \|Q - A - B_2\|^2_F$$

where B1 and B2 are updated as:

$$B1 = B1 + \nabla A^T - P$$
$$B2 = B2 + A - Q$$

Above problem is separable in each variable therefore can be written into following subproblems as

$$P1 : \min_P \mu_1 \|P - \nabla A^T - B_1\|^2_F + \lambda_1 \|P\|_1$$

$$P2 : \min_Q \mu_2 \|Q - A - B_2\|^2_F + \lambda_2 \|Q\|_{2,1}$$

$$P3 : \min_S \|Y - MA - S\|^2_F + \lambda_3 \|S\|_1$$

$$P4 : \min_A \|Y - MA - S\|^2_F + \mu_1 \|P - \nabla A^T - B_1\|^2_F + \mu_2 \|Q - A - B_2\|^2_F$$

The Bregman Iterative Algorithm has been applied to many problems including image denoising and Basis pursuit because it has some convergence properties. These properties include monotonic decrease in the residual term, convergence to the original image or signal to recover the residual term with exact data, and convergence in terms of Bregman distance to the original image or signal with noisy data. Split bregman is one of the fastest solvers for total variation denoising, image reconstruction from fourier coefficients, convex image segmentation and many other problems.

Total variation denoising, also known as total variation regularization, is a process most often used in digital image processing, that has applications in noise removal. It is based on the principle that signals with excessive and possibly spurious detail have high total variation, that is the integral of the absolute gradient of the signal is high. According to this principle, reducing the total variation of the signal subject to it being a close match to the original signal, removes unwanted detail whilst preserving important details such as edges.

This noise removal technique has advantages over simple techniques such as linear smoothing or median filtering which reduce noise but at the same time smooth away edges to a greater or lesser degree. By contrast, total variation denoising is remarkably effective at simultaneously preserving edges whilst smoothing away noise in flat regions, even at low signal-to-noise ratios.

Total variation can be seen as a non-negative real valued functional defined on the space of real-valued functions or on the space of integrable functions. As a functional, total variation finds applications in several branches of mathematics and engineering, like optimal control, numerical analysis, and calculus of variations, where the solution to a certain problem has to minimize its value.

Sparse approximation ideas and algorithms have been extensively used in signal processing, image processing, machine learning, medical imaging, array processing, data mining, and more. In most of these applications, the unknown signal of interest is modeled as a sparse combination of a few atoms from a given dictionary, and this is used as the regularization of the problem. In addition to being universally incoherent, random measurements are also future proof, if a better sparsity-inducing basis is found, then the same random measurements can be used to reconstruct an even more accurate view of the environment. The joint sparsity method exploits the end members present in the abundance maps present in the different locations of an image and also provides smoothness to the image.

DOI: 10.23883/IJRTER.CONF.20190304.005.RCLXE

Thus they allow a progressively better reconstruction of the data as more measurements are obtained, one or more measurements can also be lost without corrupting the entire reconstruction .Simple joint sparsity models capture the essence of real physical scenarios, illustrate the basic analysis and algorithmic techniques and indicate the gains to be realized from joint recovery.

Algorithm 1 Proposed JSTV Algorithm

1: Input: Y, λ_1, λ_2, μ_1, μ_2, innerIter, outerIter
2: output: A (Abundance maps)
3: **for** j =1 to outerIter **do**
4: **for** k=1 to innerIter **do**
5: $P^{K+1} = \text{SoftTh}\ (\nabla(A^k)^T + B^k{}_1, \frac{\lambda 1}{\mu 1})$
6: $Q^{k+1} = \text{Shrink}\ (A^k + B^k{}_2, \frac{\lambda 2}{\mu 2})$
7: $S^{k+1} = \text{SoftTh}\ (MA^K - Y, \lambda_3)$
8: $A^{k+1} = \text{mat}\ (a)$
9: $B_1^{k+1} = B_1^k + D_h X^{k+1} D - P^{k+1}$
10: $B_2^{k+1} = B_2^k + D_v X^{k+1} D - P^{k+1}$
11: **end for**
12: $Y = Y - MA^k - S^k$
13: **end for**
14:return $A = A^{J|1}$

IV EXPERIMENTS AND RESULTS

This section describes the details of various experiments executed to validate the proposed method. The existing USGS spectral library was utilized in all the experiments. The library contains spectral signatures under six categories namely artificial, coatings, minerals, liquids, soil, and vegetation. Each abundance map is composed of two or three endmembers as represented by the number of rectangular boxes inside a map. The synthetic data experiments were conducted to quantify the performance of proposed unmixing algorithm. The synthetic dataset was generated using HYperspectral data viewer for Development of Research Applications (HYDRA) toolbox. Dark blue background color represents zero pixel value. Both the datasets satisfy abundance sum to one constraint as well as abundance non-negativity constraint.

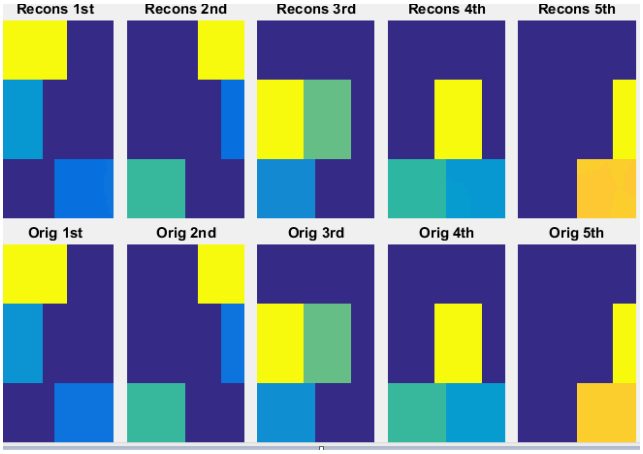

Figure1: Abundance maps of different images

The input image which is taken for analysis is synthetic hyperspectral image. The synthetic dataset has five abundance map of 50 ×50 pixels with constant fraction over a region. Each abundance map is composed of two or three endmembers as represented by the number of rectangular boxes inside a map. Abundance map shows the distribution of a particular endmember over a region. The pure pixels have the fractional abundance of one whereas mixed pixels have fractional abundance between zero and one. The total number of endmembers available from different spectral libraries are huge, but only a few of these endmembers are present in a given hyperspectral image. At every pixel, a subset of the endmembers are present.Five endmembers were randomly selected to generate first Synthetic image of dimension 50×50×224.

The original hyperspectral image is mixed with noise such as Gaussian and Sparse noise. Gaussian noise mostly occurs during image acquisition process due to poor lighting, dark current or sensor noise. The term sparse noise corresponds to the noise that affects few pixels in the image. It includes line strips, shot noise as well as impulse noise. The experiments were done on the synthetic image with mixed noise consisting of Gaussian noise and vertical line strijps. Horizontal line strips often occur in images captured by whisk-broom kind of sensors that have rotating mirrors perpendicular to the flight direction. These experiments were done to check the robustness of proposed unmixing method in the presence of different kinds of noise. The Gaussian noise of Signal to Noise Ratio (SNR) of 30 dB was added, but sparse noise is not known a priori value.

The output image is the reconstruction of the original image. Synthetic hyperspectral image clearly shows the advantage of utilizing the concept of sparse noise in the unmixing framework. Since this image has a lot of smooth regions therefore Gaussian noise can be easily spotted in denoised images however compared to other algorithms the proposed JSTV algorithm has significantly reduced both kinds of noise. The Joint Sparsity and Total Variation (JSTV) method provides the reconstruction of the abundance map by providing exact endmembers in the appropriate areas

DOI: 10.23883/IJRTER.CONF.20190304.005.RCLXE

as well as smoothens the image by removing the unwanted information and noise

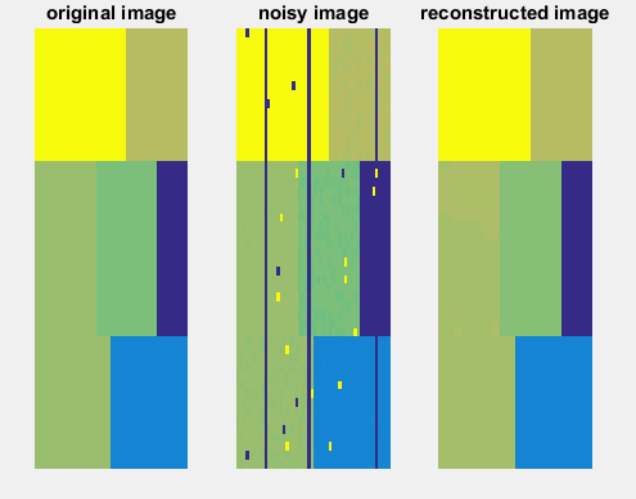

Figure2: Abundance maps estimated by JSTV

A. Evaluation Metric

PSNR between original image X and reconstructed image Y was calculated as:

$$\text{PSNR} = 10 \log_{10} \left(\frac{\max(x)2}{MSE} \right)$$

The Peak Signal to Noise Ratio (PSNR) value for a hyperspectral image was calculated as the average of the sum of PSNR value for each band. PSNR is an engineering term for the ratio between the maximum possible power of a signal and the power of corrupting noise that affects the fidelity of its representation. Because many signals have a very wide dynamic range,

```
PSNR of noisy image= 8.997199
 Elapsed time is 30.367960 seconds.

Reconstructed Abundance PSNR=41.502979
Reconstructed Image PSNR= 43.661829
```

Figure 3: PSNR and Time values for unmixed image

PSNR is usually expressed in terms of the logarithmic decibel scale. PSNR is most commonly used to measure the quality of reconstruction .The signal in this case is the original data, and the noise is the error introduced by compression. PSNR is an approximation to human perception of reconstruction quality.

The exact reconstruction will lead to the maximum value of PSNR as infinite. Higher the PSNR value better is the reconstruction quality

IV CONCLUSION

Spectral unmixing and denoising algorithms for hyperspectral remote sensing have always been considered independently. In this method, a new approach for hyperspectral unmixing has been developed. This approach exploits joint sparsity as well as the piece-wise smoothness of abundance maps in the generic noise model which explicitly account for sparse and Gaussian noise. Simultaneous utilization of both total-variation regularization and joint-sparse regularization is not redundant as both achieve different goals. Total variation regularization has explored smoothness of abundance maps whereas joint-sparsity exploit the endmember present at various locations in the same area. The results shows that by imposing total variation, the unmixing results improve significantly with latent clean image, especially in scenarios highly contaminated with noise.

Experimental results show that the proposed method provides enhanced denoising performance with respect to regular hyperspectral unmixing, while also retaining the anomalous endmembers, which may be of interest for many applications. The proposed framework utilized existing USGS spectral library for spectral signatures. The spectral signatures in the existing library can differ from the spectral signatures present in the image. This work can also be extended to derive the endmember signatures directly from the hyperspectral image. In future in order to exploit the endmembers present in the abundance map and also to improve the smoothness of the hyperspectral image another unmixing method can be proposed.

REFERENCES

[1] J. Chi and M. M. Crawford, "Spectral Unmixing-Based Crop Residue Estimation Using Hyperspectral Remote Sensing Data: A Case Study at Purdue University," IEEE J. Sel. Top. Appl. Earth Obs Remote Sens., vol. PP, no. 99, pp. 1–10, 2014.

[2] M. Hedegaard, C. Matth¨aus, S. r. Hassing, C. Krafft, M. Diem, and J. Popp, "Spectral unmixing and clustering algorithms for assessment of single cells by Raman microscopic imaging," Theor. Chem. Acc., vol. 130, no. 4-6, pp. 1249–1260, 2011

[3] I. Dopido, A. Villa, A. Plaza, and P. Gamba, "A Quantitative and Comparative Assessment of Unmixing-Based Feature Extraction Techniques for Hyperspectral Image Classification,"IEEE J. Sel. Top. Appl. Earth Obs. Remote Sens., vol. 5, no. 2, pp. 421–435, 2012.

[4] A. Ert ¨urk, "Enhanced Unmixing-Based Hyperspectral Image Denoising Using Spatial Preprocessing," IEEE J. Sel. Top. Appl. Earth Obs. Remote Sens., vol. 8, no. 6, pp. 2720–2727, 2015.

[5] S. Delalieux, P. J. Zarco-Tejada, L. Tits, M. A. J. Bello, D. S. Intrigliolo,and B. Somers, "Unmixing-based fusion of hyperspatial and hyperspectral airborne imagery for early detection of vegetation stress," IEEE J. Sel. Top . Appl. Earth Obs. Remote Sens., vol. 7, no. 6, pp. 2571–

DOI: 10.23883/IJRTER.CONF.20190304.005.RCLXE

2582,2014.
[6] Y. Gu, Y. Zhang, and J. Zhang, "Integration of spatial-spectral information for resolution enhancement in hyperspectral images," IEEE Trans. Geosci. Remote Sens.,vol. 46, no. 5, pp. 1347–1358, 2008.
[7] J. M. Bioucas-dias, A. Plaza, N. Dobigeon, M. Parente, Q. Du, P. Gader, and J. Chanussot, "Hyperspectral Unmixing Overview: Geometrical , Statistical , and Sparse Regression-Based Approaches," IEEE J. Sel. Top. Appl. Earth Obs. Remote Sens., vol. 5, no. 2, pp. 354– 379, 2012.
[8] R. Heylen, M. Parente, and P. Gader, "A review of nonlinear hyperspectral unmixing methods," IEEE J. Sel.Top. Appl. Earth Obs. Remote Sens., vol. 7, no. 6, pp 844–1868, 2014.
[9] J. W. Boardman, "Automating spectral unmixing of AVIRIS data using convex geometry concepts," in Summ. 4th Annu. JPL Airborne Geosci. Work., 1993, pp. 11–14.
[10] M. E. Winter, "N-FINDR: an algorithm for fast autonomous spectral end-member determination in hyperspectral data," in SPIE Int. Symp. Opt. Sci. Eng. Instrum., 1999, pp. 266–275.
[11] L. Miao and H. Qi, "Endmember extraction from highly mixed data using minimum volume constrained nonnegative matrix factorization," IEEE Trans. Geosci. Remote Sens., vol. 45, no. 3, pp. 765–777, 2007.
[12] D. Cerra, M. Rupert, and P. Reinartz, "Noise Reduction in Hyperspectral Images Through Spectral Unmixing," IEEE Geosci. Remote Sens. Lett., vol. 11, no. 1, pp. 109–113, 2014.
[13] Z. Zhou, X. Li, J. Wright, E. Cand`es, and Y. Ma, "Stable Principal Component Pursuit," in IEEE Int. Symp. Inf. Theory, 2010, pp. 1518–1522.
[14] H. Zhang, W. He, L. Zhang, H. Shen, and Q. Yuan, "Hyperspectral Image Restoration Using Low-Rank Matrix Recovery," IEEE Trans. Geosci. Remote Sens., vol. PP, no. 99, pp. 1–15, 2013.
[15] J. V. Shi, A. C. Sankaranarayanan, C. Studer, and R. G. Baraniuk, "Video compressive sensing for dynamic MRI," BMC Neurosci., vol. 13, no. Suppl 1, p. P183, 2012.
[16] L. I. Rudin, S. Osher, and E. Fatemi, "Nonlinear Total Variation Based Noise Removal Algorithms," Phys. D Nonlinear Phenom., vol. 60, no. 1, pp. 259–268, 1992.
[17] T. Goldstein and S. Osher, "The Split Bregman Method for L1-Regularized Problems," SIAM J. Imaging Sci., vol. 2, no. 2, pp. 323–343, Jan. 2009.
[18] J. M. Bioucas-dias and M. A. T. Figueiredo, "Alternating Direction Algorithmsfor Constrained Sparse Regression: Application to Hyperspectral Unmixing," in Work. Hyperspectral Image Signal Process. Evol. Remote Sens., 2010, pp. 1–4.
[19] M.-d. Iordache, J. M. Bioucas-dias, and A. Plaza, "Total Variation Spatial Regularization for Sparse Hyperspectral Unmixing," IEEE Trans. Geosci. Remote Sens., vol. 50, no. 11, pp. 4484–4502, 2012.
[20] "Collaborative Sparse Regression for Hyperspectral Unmixing,"IEEE Trans. Geosci. Remote Sens., vol. 52, no. 1, pp. 341–354, 2014.
[21] M.-D. Iordache, J. M. Bioucas Dias, and A. Plaza, "Sparse Unmixing of Hyperspectral Data," IEEE Trans. Geosci. Remote Sens., vol. 49, no. 6, pp. 2014–2039, 2011.
[22] Q. Qu, N. M. Nasrabadi, and T. D. Tran, "Abundance Estimation for Bilinear Mixture Models via Joint Sparse and Low-Rank Representation," IEEE Trans. Geosci.Remote Sens., vol. 52, no. 7, pp. 4404–4423, 2014.
[23] D. Donoho, "Compressed sensing," IEEE Trans. Inf. Theory, vol. 52, no. 4, pp. 1289–1306, Apr. 2006.
[24] E. Candes, J. Romberg, and T. Tao, "Stable Signal Recovery from Incomplete and Inaccurate Measurements," Commun. Pure Appl. Math., vol. 59, no. 8, pp. 1207–1223, 2006.
[25] B. K. Natarajan, "Sparse approximate solutions to linear Systems," SIAM J. Comput., vol. 24, no. 2, pp. 227–234, 1995.

